STATISTICS, OPTIMIZATION AND INFORMATION COMPUTING
Stat., Optim. Inf. Comput., Vol. **15**, June 2026, pp 5170–5192.
Published online in International Academic Press (www.IAPress.org)

Restricted Additive Schwarz Algorithm for a θ Finite Difference Method to Solve a Two-dimensional 4th-order Partial Differential Equation with Variable Coefficient

Chadi CHAHID[1,*], Yassin KHALI [2], Samir KHALLOUQ [1], Nabila NAGID[3]

[1] *Laboratory of Mathematics and Interactions, Faculty of Sciences, Moulay Ismaïl University, Morocco*
[2] *Laboratory of Mathematics and Interactions, Faculty of Sciences and Techniques, Moulay Ismaïl University, Morocco*
[3] *Laboratory of Mathematics, Modeling and Automatic Systems, Faculty of Sciences Semlalia, Cadi Ayyad University, Morocco*

Abstract This paper deals with a θ finite difference scheme to solve two-dimensional 4th-order partial differential equation with variable coefficient, which governs the transverse vibrations of a thin plate. First we establish some a priori estimates for the weak solution of our problem. Then, we introduce a new variable, allowing us to convert the plate equation into a system of two second-order differential equations. Stability and convergence analysis are carried out by employing the energy estimate method. We present a class of domain decomposition methods (DDM) called restricted additive Schwarz (RAS). This method is used as a preconditioner for the GMRES algorithm to solve systems of linear equations arising from the discretization of the plate equation by the present scheme. Numerical experiments are provided, confirming the effectiveness of the algorithms.

Keywords Thin plate, 4th-order partial differential equation, Finite differences method, Stability analysis, Convergence analysis, Domain decomposition methods, Restricted additive Schwarz, Preconditioning, Parallel computing

AMS 2010 subject classifications 65M06, 65M12, 65M22, 65M55, 65Y05

DOI: 10.19139/soic-2310-5070-3021

1. Introduction

We consider the transverse deflection of a simply supported thin plate governed by the following two-dimensional 4th-order partial differential equation with variable coefficient of the form,

$$\frac{\partial^2 u}{\partial t^2} + a(x,y)\left(\frac{\partial^4 u}{\partial x^4} + 2\frac{\partial^4 u}{\partial x^2 \partial y^2} + \frac{\partial^4 u}{\partial y^4}\right) = f(x,y,t), \quad (x,y) \in \Omega,\ 0 < t \leq T, \tag{1}$$

where $\Omega = \{(x,y) \mid\ L_0 < x, y < L_1\} \subset \mathbb{R}^2$ is a bounded spatial domain with boundary Γ, $T > 0$, $u(x,y)$ is the transverse deflection, and $f(x,y,t)$ is the applied transverse loading at point (x,y) and time t. The variable coefficient $a = a(x,y)$ is assumed to satisfy

$$0 < a_0 \leq a(x,y) \leq a_1 < +\infty, \quad (x,y) \in \Omega, \tag{2}$$

with a_0 and a_1 being constants.

*Correspondence to: Chahid CHADI (Email: ch.chahid@edu.umi.ac.ma). Department of Mathematics, Faculty of Sciences (FSM), Moulay Ismaïl University. Morocco

ISSN 2310-5070 (online) ISSN 2311-004X (print)

Equation (1) is supplemented with the following initial conditions

$$\begin{cases} u(x,y,0) = u_0(x,y), & L_0 \le x,y \le L_1, \\ \dfrac{\partial u(x,y,0)}{\partial t} = \psi_0(x,y), & L_0 \le x,y \le L_1, \end{cases} \tag{3}$$

where u_0 and ψ_0 are the initial deflection and initial velocity, respectively. We consider the following boundary conditions:

$$\begin{cases} u(L_0,y,t) = g_1(y,t), \quad u(L_1,y,t) = g_2(y,t), & L_0 \le y \le L_1, \quad 0 < t \le T, \\ u(x,L_0,t) = g_3(x,t), \quad u(x,L_1,t) = g_4(x,t), & L_0 \le x \le L_1, \quad 0 < t \le T, \\ \dfrac{\partial^2 u(L_0,y,t)}{\partial x^2} = h_1(y,t), \quad \dfrac{\partial^2 u(L_1,y,t)}{\partial x^2} = h_2(y,t), & L_0 \le y \le L_1, \quad 0 < t \le T, \\ \dfrac{\partial^2 u(x,L_0,t)}{\partial y^2} = h_3(x,t), \quad \dfrac{\partial^2 u(x,L_1,t)}{\partial y^2} = h_4(x,t), & L_0 \le x \le L_1, \quad 0 < t \le T. \end{cases} \tag{4}$$

Equation (1) is commonly used to describe the vibration problems related to thin plate structures. These structures play a central role in various industrial sectors, such as civil engineering, automotive, aerospace, and aeronautics. Solving 4th-order PDEs by analytical methods is extremely complex and difficult in most cases; it is necessary instead to use numerical approaches. A number of numerical methods have been proposed to solve the Equation (1). The finite difference method has proved very attractive because of its flexibility and robustness in producing highly accurate solutions. Many authors such as Crandall [14], Conte [13], Gourlay [18], Twizell and Khaliq [31], have successfully used finite difference methods to solve 4th-order PDEs. In addition, compact difference schemes have been applied successfully to solve 4th-order PDEs, for example, the authors in [1] solved a one-dimensional 4th-order differential equation using a compact finite difference scheme for the spatial derivative and a second-order Crank–Nicolson approximation for the temporal derivative. Mohanty and Kaur [27] proposed a compact finite difference scheme for Equation (1) with a convergence rate of $\mathcal{O}(\tau^2 + h^4)$. In [22], the authors used a combination of a proper orthogonal decomposition with a compact finite difference scheme to solve Equation (1). According to the results in [1, 22, 27], the compact finite difference schemes indeed provide very high spatial accuracy to solve Equation (1) with constant coefficient. However, to the best of our knowledge, stability and convergence results for variable coefficient problem is still an issue. A high-order compact difference scheme to solve a two-dimensional nonlinear 4th-order equation was presented in [21]. Spline functions have also been employed in getting the numerical solution of many types of PDEs, For example, Çağlar et al. [9] considered a family of B-spline methods for solving a 4th-order non-homogeneous PDE. Aziz et al. [2] have developed a three-level method based on a parametric spatial quintic spline and finite difference discretization in time to solve a 4th-order non-homogeneous PDE. A numerical scheme based on sextic B-spline for a 4th-order PDE was presented by Mohammadi in [26]. The author used finite difference method and a sextic B-spline method on uniform meshes. Mittal et al. [25], have presented two numerical methods based on cubic B-spline to approximate the spatial derivative appearing in a 4th-order PDE, for the time derivative, the authors have used the forward difference approximation. In the work [11], the authors have solved a 4th-order nonlinear variable coefficient equation using a Crank–Nicolson mixed finite-element scheme combined with the proper orthogonal decomposition technique, which remarkably reduced the CPU time.

In this paper, we present a numerical scheme to solve the 4th-order Equation (1) with variable coefficient, using a finite difference spatial scheme combined with a time $\theta-$scheme. Stability analyses for constant coefficient discretizations are often carried out using Fourier analysis. Since this technique does not extend to variable coefficient problems, we prove the stability and convergence using the energy method. The convergence order of the proposed scheme is second order both in temporal and spatial directions, but solving at each time step the

il-conditioned linear system resulting from the discretization of Equation (1) via our scheme is a difficult task, since its condition number is of order $\mathcal{O}(h^{-4})$, growing fast and unboundedly when the mesh size h approaches 0. Therefore, the classical iterative methods or direct methods are not suitable in this case. Instead, it is very important to employ an advanced iterative solver and construct a proper preconditioner, which can significantly reduce the condition number in the equivalent preconditioned linear system.

We consider domain decomposition methods (DDMs) as parallel preconditioners for the 4th-order Equation (1). DDMs are nowadays found to be highly efficient and widely adopted to solve algebraic systems obtained from the discretization of many types of partial differential equations (PDEs) [3, 4, 5, 7, 29]. Various domain decomposition algorithms have been developed and analyzed, such as the additive Schwarz (AS) method [16], and the restricted additive Schwarz (RAS) method [10]. These methods were further analyzed in [15, 24, 30]. The RAS method is a parallel domain decomposition method and has shown better performance compared to the other DDM methods in terms of number of iterations and CPU time (see [17]). The work in [6] presented synchronous and asynchronous RAS methods accelerated with the epsilon algorithm, resulting in further computational cost reductions. Our focus here is to employ the RAS method as a preconditioner for the GMRES method, which improves its convergence when solving the 4th-order partial differential Equation (1).

Our paper is organized as follows. In Section 2 we derive some a priori estimates for the weak solution of the Equations (1)-(4). In Section 3, we construct the finite difference scheme combined with the time $\theta-$scheme for Equation (1). In Section 4, we analysis the stability and convergence of the proposed scheme in the l^2-norm. In Section 5, we present and apply the RAS preconditioner to solve the discrete problem. In Section 6, two numerical experiments are presented to verify the theoretical findings and confirm the effectiveness of the RAS preconditioner. Section 7 is for the concluding remark.

2. Estimates for the weak solution of (1)-(4)

For any function $\varphi = \varphi(x, y, t)$, we denote by $\varphi(t)$, the function $\varphi(t) : (x, y) \in \Omega \longmapsto \varphi(x, y, t),\ t \in [0, T]$. According to [12], for any initial data $u_0 \in H^2(\Omega)$ and $\psi_0 \in L^2(\Omega)$, the problem (1)-(4) admits a weak solution $u \in L^2(0, T; H)$, where $H = \left\{v \in H^2(\Omega);\ v = 0 \text{ on } \partial\Omega\right\}$, In addition, we have the following result:

Theorem 2.1
We assume homogeneous boundary conditions, $u_0 \in H^2(\Omega)$ and $\psi_0 \in L^2(\Omega)$, then the weak solution of the Problem (1)-(4) satisfies the following estimates:

$$\|\Delta u(t)\|_{L^2(\Omega)} \leq C, \text{ and } \left\|\frac{\partial u(t)}{\partial t}\right\|_{L^2(\Omega)} \leq C,$$

where $C > 0$ is a constant independent of t.

Proof
Consider the potential energy $E_u(t)$ of the system (1)-(4) given by

$$E_u(t) = \frac{1}{2}\int_\Omega |\Delta u(t)|^2 dxdy + \frac{1}{2}\int_\Omega a^{-1}\left|\frac{\partial u(t)}{\partial t}\right|^2 dxdy. \tag{5}$$

We have,

$$\frac{d}{dt}E_u(t) = \frac{1}{2}\int_\Omega \frac{\partial|\Delta u(t)|^2}{\partial t}dxdy + \frac{1}{2}\int_\Omega a^{-1}\frac{\partial}{\partial t}\left|\frac{\partial u(t)}{\partial t}\right|^2 dxdy,$$

$$= \int_\Omega \Delta u(t)\Delta\left(\frac{\partial u(t)}{\partial t}\right)dxdy + \int_\Omega a^{-1}\frac{\partial u(t)}{\partial t}\frac{\partial^2 u(t)}{\partial t^2}dxdy,$$

$$= \int_\Omega \Delta^2 u(t)\frac{\partial u(t)}{\partial t}dxdy - \int_\Gamma\left(\frac{\partial u(t)}{\partial t}\frac{\partial(\Delta u(t))}{\partial \boldsymbol{n}} - \Delta u(t)\frac{\partial}{\partial \boldsymbol{n}}\left(\frac{\partial u(t)}{\partial t}\right)\right)d\Gamma + \int_\Omega a^{-1}\frac{\partial u(t)}{\partial t}\frac{\partial^2 u(t)}{\partial t^2}dxdy,$$

$$= \int_\Omega\left(\Delta^2 u(t) + a^{-1}\frac{\partial^2 u(t)}{\partial t^2}\right)\frac{\partial u(t)}{\partial t}dxdy - \int_\Gamma\left(\frac{\partial u(t)}{\partial t}\frac{\partial(\Delta u(t))}{\partial \boldsymbol{n}} - \Delta u(t)\frac{\partial}{\partial \boldsymbol{n}}\left(\frac{\partial u(t)}{\partial t}\right)\right)d\Gamma,$$

$$= \int_\Omega a^{-1}f(t)\frac{\partial u(t)}{\partial t}dxdy + \int_\Gamma\left(\frac{\partial u(t)}{\partial t}\frac{\partial(\Delta u(t))}{\partial \boldsymbol{n}} - \Delta u(t)\frac{\partial}{\partial \boldsymbol{n}}\left(\frac{\partial u(t)}{\partial t}\right)\right)d\Gamma.$$

where $\partial/\partial\boldsymbol{n}$ is the outward normal derivative on Γ. We then obtain:

$$\frac{d}{dt}E_u(t) = \int_\Omega a^{-1}f(t)\frac{\partial u(t)}{\partial t}dxdy,$$

Then, using Cauchy-Schwarz inequality, we obtain

$$\frac{d}{dt}E_u(t) \le \frac{1}{2a_0^2}\int_\Omega |f(t)|^2 dxdy + \frac{1}{2}\int_\Omega\left|\frac{\partial u(t)}{\partial t}\right|^2 dxdy,$$

then,

$$\frac{d}{dt}E_u(t) \le \frac{1}{2a_0^2}\|f(t)\|^2_{L^2(\Omega)} + a_1 E_u(t).$$

Applying Gronwall inequality, we have for all $t > 0$, the following energy identity

$$E_u(t) \le \underbrace{\left(E_u(0) + \frac{1}{2a_0^2}\int_0^T \|f(t)\|^2_{L^2(\Omega)}dt\right)}_{C}\exp(a_1 T), \tag{6}$$

where, $E_u(0)$ is giving by:

$$E_u(0) = \frac{1}{2}\left\|\Delta u_0\right\|^2_{L^2(\Omega)} + \frac{1}{2}\left\|\sqrt{a^{-1}}\psi_0\right\|^2_{L^2(\Omega)}.$$

The desired estimations follows immediately using (5) and (6), which completes the proof. □

3. Description of the θ finite difference method

We first introduce an additional variable v defined by $v = -\nabla^2 u$, where ∇^2 stands for the Laplace operator $\left(\text{i.e.,}\nabla^2 = \frac{\partial^2}{\partial x^2} + \frac{\partial^2}{\partial y^2}\right)$, then Equation (1) can be converted into a system of two second-order equations:

$$\begin{cases} \dfrac{\partial^2 u}{\partial t^2} - a(x,y)\left(\dfrac{\partial^2 v}{\partial x^2} + \dfrac{\partial^2 v}{\partial y^2}\right) = f(x,y,t), \quad (x,y)\in\Omega, \text{ and } 0 < t \le T, & (7) \\ v + \left(\dfrac{\partial^2 u}{\partial x^2} + \dfrac{\partial^2 u}{\partial y^2}\right) = 0, \quad (x,y)\in\Omega, \text{ and } 0 < t \le T. & (8) \end{cases}$$

For a numerical solution of the system (7)-(8), we partition the spatial domain Ω using the grid points

$$(x_i, y_j) = (ih, jh),\ i = 0, \ldots, N,\ j = 0, \ldots, N,$$

where $h = 1/N$ is the step size of the space variables x and y and $N \in \mathbb{N}$. Let $\tau = \frac{T}{J}$ denotes the step size of the time variable t, and define $t_n = n \times \tau$, for $n = 0, 1, \ldots, J$, with $J \in \mathbb{N}$. Let at the grid points (x_i, y_j, t_n), the exact solution values of $u(x, y, t)$ and $v(x, y, t)$, be denoted by u_{ij}^n and v_{ij}^n. and the approximate solution values by U_{ij}^n and V_{ij}^n, respectively. We assume that the exact solution $u(x, y, t)$, initial and boundary conditions are sufficiently regular to achieve and conserve the order of accuracy of the finite difference approximations. We consider the following space and time difference operators:

Table 1. Space and time difference operators

Operator	Formula
$\delta_x^2 u_{ij}$	$\frac{u_{i+1,j} - 2u_{i,j} + u_{i-1,j}}{h^2}$
$\delta_y^2 u_{ij}$	$\frac{u_{i,j+1} - 2u_{i,j} + u_{i,j-1}}{h^2}$
$A_h u_{ij}$	$-\left(\delta_x^2 u_{ij} + \delta_y^2 u_{ij}\right)$
$\delta_t^2 u_{ij}^n$	$\frac{u_{i,j}^{n+1} - 2u_{i,j}^n + u_{i,j}^{n-1}}{h^2}$

By Taylor expansion in time, we obtain for the second-order time derivative in (7),

$$\frac{\partial^2 u_{ij}^n}{\partial t^2} = \delta_t^2 u_{ij}^n - \frac{\tau^2}{12}\frac{\partial^4 u_{ij}^n}{\partial t^4} - \frac{\tau^4}{360}\frac{\partial^6 u_{ij}^n}{\partial t^6} + \mathcal{O}(\tau^6), \tag{9}$$

We then apply the Taylor expansion in time to the second-order spatial derivatives in (7), and we get,

$$\frac{\partial^2 v_{ij}^n}{\partial x^2} = \frac{\partial^2 v_{ij}^{n+\theta}}{\partial x^2} - \theta\tau^2\frac{\partial^4 v_{ij}^n}{\partial t^2 \partial x^2} - \theta\tau^4\frac{\partial^6 v_{ij}^n}{\partial t^4 \partial x^2} + \mathcal{O}(\tau^6), \tag{10}$$

$$\frac{\partial^2 v_{ij}^n}{\partial y^2} = \frac{\partial^2 v_{ij}^{n+\theta}}{\partial y^2} - \theta\tau^2\frac{\partial^4 v_{ij}^n}{\partial t^2 \partial y^2} - \theta\tau^4\frac{\partial^6 v_{ij}^n}{\partial t^4 \partial y^2} + \mathcal{O}(\tau^6). \tag{11}$$

Where we have denoted $\varphi^{n+\theta} = \theta\varphi^{n+1} + (1 - 2\theta)\varphi^n + \theta\varphi^{n-1}$, for any function φ and $0 \leq \theta \leq 1$.
Substituting the equations (9)-(11) into the Equation (7) evaluated at (x_i, y_j, t_n), yields:

$$\delta_t^2 u_{ij}^n - a_{ij}\Delta v_{ij}^{n+\theta} = f_{ij}^{n+\theta} + s_{ij}^n, \tag{12}$$

where

$$s_{ij}^n = \frac{\tau^2}{12}\frac{\partial^4 u_{ij}^n}{\partial t^4} + \frac{\tau^4}{360}\frac{\partial^6 v_{ij}^n}{\partial t^6} - a_{ij}\theta\tau^2\frac{\partial^2\left(\Delta v_{ij}^n\right)}{\partial t^2} - a_{ij}\theta\tau^4\frac{\partial^4\left(\Delta v_{ij}^n\right)}{\partial t^4} - \theta(f_{ij}^{n+1} - 2f_{ij}^n + f_{ij}^{n-1}) + \mathcal{O}(\tau^6), \tag{13}$$

Since u_{ij}^n is the exact solution of (7), it follows that

$$s_{ij}^n = \tau^2\left(\frac{1}{12} - \theta\right)\frac{\partial^4 u_{ij}^n}{\partial t^4} - \theta\frac{\tau^4}{12}\frac{\partial^4 f_{ij}^n}{\partial t^4} + \frac{\tau^4}{360}\frac{\partial^6 v_{ij}^n}{\partial t^6} - a_{ij}\theta\tau^4\frac{\partial^4\left(\Delta v_{ij}^n\right)}{\partial t^4} + \mathcal{O}(\tau^6). \tag{14}$$

Hence,

$$s_{ij}^n = \tau^2\left(\frac{1}{12} - \theta\right)\frac{\partial^4 u_{ij}^n}{\partial t^4} + \mathcal{O}(\tau^4), \tag{15}$$

In order to achieve second-order accuracy in space, in Equation (12), we apply the Taylor expansion for the space derivatives, and we get

$$\Delta v_{ij}^{n+\theta} = \delta_x^2 v_{ij}^{n+\theta} + \delta_y^2 v_{ij}^{n+\theta} - \frac{h^2}{12}\left(\frac{\partial^4 v_{ij}^{n+\theta}}{\partial x^4} + \frac{\partial^4 v_{ij}^{n+\theta}}{\partial y^4}\right) + \mathcal{O}(h^4), \tag{16}$$

Hence (12) can be rewritten as:

$$\delta_t^2 u_{ij}^n - a_{ij}\left(\delta_x^2 v_{ij}^{n+\theta} + \delta_y^2 v_{ij}^{n+\theta}\right) = f_{ij}^{n+\theta} + T_{ij,1}^n \tag{17}$$

where

$$T_{ij,1}^n = s_{ij}^n - a_{ij}\frac{h^2}{12}\left(\frac{\partial^4 \bar{v}_{ij}^{n+\theta}}{\partial x^4} + \frac{\partial^4 \bar{v}_{ij}^{n+\theta}}{\partial y^4}\right) + \mathcal{O}(h^4). \tag{18}$$

Canceling the higher-order terms in (18), yields

$$T_{ij,1}^n = s_{ij}^n + \mathcal{O}(h^2), \tag{19}$$

Similarly, by considering the Equation (8) at (x_i, y_j, t_n), it can be rewritten as:

$$v_{ij}^n + \left(\delta_x^2 + \delta_y^2\right) u_{ij}^n = T_{ij,2}^n = \mathcal{O}(h^2). \tag{20}$$

Finally, replacing u_{ij}^n and v_{ij}^n by their approximations U_{ij}^n, V_{ij}^n, respectively, we arrive at the the following fully discrete scheme,

$$\begin{cases} \delta_t^2 U_{ij}^n - a_{ij}\left(\delta_x^2 V_{ij}^{n+\theta} + \delta_y^2 V_{ij}^{n+\theta}\right) = f_{ij}^{n+\theta}, \text{ for } i,\ j = 1, \ldots, N-1, \text{ and } n = 1, \ldots, J, & (21) \\ V_{ij}^n + \left(\delta_x^2 + \delta_y^2\right) U_{ij}^n = 0, \text{ for } i,\ j = 1, \ldots, N-1, \text{ and } n = 1, \ldots, J. & (22) \end{cases}$$

In order to represent (21)-(22) in matrix–vector form, for any function φ, we let:

$$\boldsymbol{\varphi_h} = \left(\tilde{\boldsymbol{\varphi}}_{\mathbf{1}}, \tilde{\boldsymbol{\varphi}}_{\mathbf{2}}, \tilde{\boldsymbol{\varphi}}_{\mathbf{3}}, \ldots, \tilde{\boldsymbol{\varphi}}_{\boldsymbol{N-1}}\right)^T,$$

where

$$\tilde{\boldsymbol{\varphi}}_{\boldsymbol{j}} = \left(\varphi_{1,j}, \varphi_{2,j}, \varphi_{3,j}, \ldots, \varphi_{N-1,j}\right)^T \quad \text{for all } j = 1, \ldots, N-1.$$

Consider the following matrices defined by

$$\boldsymbol{A}_h = \begin{bmatrix} \boldsymbol{T}_h & I & & & \\ I & \boldsymbol{T}_h & I & & \\ & \ddots & \ddots & \ddots & \\ & & \ddots & \ddots & I \\ & & & I & \boldsymbol{T}_h \end{bmatrix}, \qquad \boldsymbol{M}_h = \begin{bmatrix} \boldsymbol{M}_1 & & & & \\ & \boldsymbol{M}_2 & & & \\ & & \ddots & & \\ & & & \ddots & \\ & & & & \boldsymbol{M}_{N-1} \end{bmatrix}.$$

The matrix I is the identity matrix of order $N-1$, $\boldsymbol{T}_h$ and $\boldsymbol{M}_j$(for $j = 1, \ldots, N-1$) are matrices of order $N-1$ defined by

$$\boldsymbol{T}_h = tri\left[\frac{-1}{h^2}, \frac{2}{h^2}, \frac{-1}{h^2}\right],\ \boldsymbol{M}_j = diag\left[\frac{1}{a_{1,j}}, \frac{1}{a_{2,j}}, \ldots, \frac{1}{a_{N-1,j}}\right],$$

where $diag(\boldsymbol{\varphi}_h)$ denotes a diagonal matrix formed from the vector $\boldsymbol{\varphi}_h$, and $tri\,[b_1, b_2, b_3]$ denotes the tridiagonal matrix with the diagonal values is b_2, the subdiagonal and superdiagonal values are b_1 and b_3, respectively. Note that $\boldsymbol{A}_h$ is the matrix representation of the difference operator A_h. Both $\boldsymbol{A}_h$ and $\boldsymbol{M}_h$ are of order $(N-1)^2$.

Then, writing (21)-(22) in matrix–vector form yields:

$$\begin{cases} \boldsymbol{M}_h \delta_t^2 \boldsymbol{U}_h^n + \boldsymbol{A}_h \boldsymbol{V}_h^{n+\theta} = \boldsymbol{M}_h \boldsymbol{f}_h^{n+\theta} + \boldsymbol{C}_h^n, & (23) \\ \boldsymbol{V}_h^n - \boldsymbol{A}_h \boldsymbol{U}_h^n = \boldsymbol{R}_h^n, & (24) \end{cases}$$

The discretized initial conditions are given by

$$u_{ij}^0 = u_0(x_i, y_j), \tag{25}$$

$$u_{ij}^1 = u_0(x_i, y_j) + \tau\psi_0(x_i, y_j) - \frac{\tau^2}{2} a_{ij} \left(\Delta^2 u_0(x_i, y_j)\right) + \frac{\tau^2}{2} f(x_i, y_j, 0) - \frac{\tau^3}{6} a_{ij} \left(\Delta^2 \psi_0(x_i, y_j)\right) + \frac{\tau^3}{6} \frac{\partial f(x_i, y_j, 0)}{\partial t}, \tag{26}$$

with $i,\ j = 0, \ldots, N$. The right-hand side vectors $\boldsymbol{R}_h$ and $\boldsymbol{C}_h$ are of order $(N-1)^2$, consisting of the boundary conditions values. Using Taylor expansion in time and the two equations (7) and (8), it can be seen that the error of the approximation (26) is of order $\mathcal{O}(\tau^4)$. Note that the choice of $\theta = 0$ in (23)-(26) leads to an explicit scheme, and $\theta \neq 0$ leads to an implicit scheme.

4. Stability and convergence analyze in l^2-norm

We next show the stability and convergence in the discrete l^2-norm of the θ Scheme (23)-(26), using the energy method. We define the following discrete spaces $\mathcal{V}_h$ and $\mathcal{V}_{h,0}$ as follows

$$\mathcal{V}_h = \{\boldsymbol{U}_h \equiv (U_{ij})\ ;\ i, j = 0, \ldots, N\},$$

$$\mathcal{V}_{h,0} = \{\boldsymbol{U}_h \in \mathcal{V}_h;\ U_{0j} = U_{Nj} = U_{i0} = U_{iN} = 0,\ i, j = 0, \ldots, N\}.$$

For each $\boldsymbol{U}_h, \boldsymbol{W}_h \in V_{h,0}$, define the following discrete l^2 inner products and corresponding norms

$$\langle \boldsymbol{U}_h\ ,\ \boldsymbol{W}_h \rangle = h^2 \sum_{i,j=1}^{N-1} U_{ij} \times W_{ij}, \qquad ||\boldsymbol{U}_h||^2 = \langle \boldsymbol{U}_h, \boldsymbol{U}_h \rangle, \tag{27}$$

$$\langle \delta_x^2 \boldsymbol{U}_h\ ,\ \delta_x^2 \boldsymbol{W}_h \rangle = h^2 \sum_{i,j=1}^{N-1} \delta_x^2 U_{i,j} \times \delta_x^2 W_{i,j}, \qquad ||\delta_x^2 \boldsymbol{U}_h||^2 = \langle \delta_x^2 \boldsymbol{U}_h, \delta_x^2 \boldsymbol{U}_h \rangle, \tag{28}$$

$$\langle \boldsymbol{A}_h \boldsymbol{U}_h, \boldsymbol{A}_h \boldsymbol{W}_h \rangle = h^2 \sum_{i,j=1}^{N-1} (A_h U_{ij}) \times (A_h W_{ij}), \qquad ||\boldsymbol{A}_h \boldsymbol{U}_h||^2 = \langle \boldsymbol{A}_h \boldsymbol{U}_h, \boldsymbol{A}_h \boldsymbol{U}_h \rangle, \tag{29}$$

and let in the sequel C means a general positive constant, which have different meaning in different places. The following lemmas and propositions will be used in the study of stability and convergence analysis of the Scheme (23)-(26).

Lemma 4.1 ([32])
For any $\boldsymbol{U}_h, \boldsymbol{W}_h \in \mathcal{V}_{h,0}$, we have $\langle \boldsymbol{A}_h \boldsymbol{U}_h, \boldsymbol{W}_h \rangle = \langle \boldsymbol{U}_h, \boldsymbol{A}_h \boldsymbol{W}_h \rangle$.

Lemma 4.2 (Discrete Gronwall's lemma [23])
Suppose that $\{E^k,\ k \geq 0\}$ and $\{g^k,\ k \geq 0\}$ are two non-negative sequences and $\Psi^0 \geq 0$. If

$$E^k \leq \Psi^0 + \tau \sum_{n=0}^{k-1} E^n + \tau \sum_{n=0}^{k} g^n,\ k \geq 0,$$

then E^k satisfies $E^k \leq e^{k\tau} \left(\Psi^0 + \tau \sum_{n=0}^{k} g^n \right),\ k \geq 0.$

Lemma 4.3
For any $\boldsymbol{U}_h \in V_{h,0}$, we have $\langle \boldsymbol{A}_h^2 \boldsymbol{U}_h, \boldsymbol{U}_h \rangle \leq \frac{64}{h^4} \|\boldsymbol{U}_h\|^2$, with $\boldsymbol{A}_h^2 \boldsymbol{U}_h = \boldsymbol{A}_h(\boldsymbol{A}_h \boldsymbol{U}_h)$.

Proof

The proof follows easily by expanding the scalar product $\langle A_h^2 \boldsymbol{U_h}, \boldsymbol{U_h} \rangle$, then applying the inequality $ab \leq \frac{a^2}{2} + \frac{b^2}{2}$, so that each term can be estimated by the bound $\|\boldsymbol{U_h}\|^2$ which lead to the desired inequality. □

Proposition 4.1
Let $(\boldsymbol{U}_h^n, \boldsymbol{V}_h^n) \in V_{h,0} \times V_{h,0}$ be the solution of the Scheme (23)-(26), and consider for $n = 0, 1, \ldots, J$, the following discrete energy denoted by $\boldsymbol{\mathcal{E}}_{uv}^{h,n+\frac{1}{2}}$,

$$\boldsymbol{\mathcal{E}}_{uv}^{h,n+\frac{1}{2}} = \frac{1}{2}\Big\langle (\boldsymbol{M}_h + \theta\tau^2 \boldsymbol{A}_h^2) \frac{\boldsymbol{U}_h^{n+1} - \boldsymbol{U}_h^n}{\tau}, \frac{\boldsymbol{U}_h^{n+1} - \boldsymbol{U}_h^n}{\tau} \Big\rangle + \frac{1}{2}\Big\langle \boldsymbol{A}_h \boldsymbol{V}_h^n, \boldsymbol{U}_h^{n+1} \Big\rangle, \tag{30}$$

we obtain

1. If $\frac{1}{4} \leq \theta \leq 1$, then the quantity $\boldsymbol{\mathcal{E}}_{uv}^{h,n+\frac{1}{2}}$ is non-negative, and satisfies the following inequality

$$\boldsymbol{\mathcal{E}}_{uv}^{h,n+\frac{1}{2}} \geq \frac{1}{2a_1} \left\| \frac{\boldsymbol{U}_h^{n+1} - \boldsymbol{U}_h^n}{\tau} \right\|^2. \tag{31}$$

2. For $0 \leq \theta < \frac{1}{4}$, under the following CFL condition:

$$\alpha := \frac{4\sqrt{a_1}\tau}{h^2} \leq \frac{1}{\sqrt{2(1-4\theta)}}, \tag{32}$$

$\boldsymbol{\mathcal{E}}_{uv}^{h,n+\frac{1}{2}}$ is also non-negative, with the following inequality holds

$$\boldsymbol{\mathcal{E}}_{uv}^{h,n+\frac{1}{2}} \geq \frac{1}{2a_1} \left(1 + (4\theta - 1)\alpha^2\right) \left\| \frac{\boldsymbol{U}_h^{n+1} - \boldsymbol{U}_h^n}{\tau} \right\|^2. \tag{33}$$

Proof

1. We have,

$$\begin{aligned}
\boldsymbol{\mathcal{E}}_{uv}^{h,n+\frac{1}{2}} &= \frac{1}{2}\Big\langle (\boldsymbol{M}_h + \theta\tau^2 \boldsymbol{A}_h^2) \frac{\boldsymbol{U}_h^{n+1} - \boldsymbol{U}_h^n}{\tau}, \frac{\boldsymbol{U}_h^{n+1} - \boldsymbol{U}_h^n}{\tau} \Big\rangle + \frac{1}{2}\Big\langle \boldsymbol{A}_h \boldsymbol{V}_h^n, \boldsymbol{U}_h^{n+1} \Big\rangle, \\
&= \frac{1}{2}\Big\langle (\boldsymbol{M}_h + \theta\tau^2 \boldsymbol{A}_h^2) \frac{\boldsymbol{U}_h^{n+1} - \boldsymbol{U}_h^n}{\tau}, \frac{\boldsymbol{U}_h^{n+1} - \boldsymbol{U}_h^n}{\tau} \Big\rangle + \frac{1}{8}\Big\langle \boldsymbol{A}_h^2 (\boldsymbol{U}_h^{n+1} + \boldsymbol{U}_h^n), \boldsymbol{U}_h^{n+1} + \boldsymbol{U}_h^n \Big\rangle \\
&\qquad - \frac{1}{8}\Big\langle \boldsymbol{A}_h^2 (\boldsymbol{U}_h^{n+1} - \boldsymbol{U}_h^n), \boldsymbol{U}_h^{n+1} - \boldsymbol{U}_h^n \Big\rangle,
\end{aligned}$$

Then,

$$\begin{aligned}
\boldsymbol{\mathcal{E}}_{uv}^{h,n+\frac{1}{2}} = \frac{1}{2}\Big\langle \left(\boldsymbol{M}_h + (\theta - \frac{1}{4})\tau^2 \boldsymbol{A}_h^2 \right) \frac{\boldsymbol{U}_h^{n+1} - \boldsymbol{U}_h^n}{\tau}, \frac{\boldsymbol{U}_h^{n+1} - \boldsymbol{U}_h^n}{\tau} \Big\rangle \\
+ \frac{1}{8}\Big\langle \boldsymbol{A}_h^2 (\boldsymbol{U}_h^{n+1} + \boldsymbol{U}_h^n), \boldsymbol{U}_h^{n+1} + \boldsymbol{U}_h^n \Big\rangle.
\end{aligned} \tag{34}$$

Using Lemma 4.1, we obtain that

$$\Big\langle \boldsymbol{A}_h^2 (\boldsymbol{U}_h^{n+1} + \boldsymbol{U}_h^n), \boldsymbol{U}_h^{n+1} + \boldsymbol{U}_h^n \Big\rangle = \Big\langle \boldsymbol{A}_h (\boldsymbol{U}_h^{n+1} + \boldsymbol{U}_h^n), \boldsymbol{A}_h (\boldsymbol{U}_h^{n+1} + \boldsymbol{U}_h^n) \Big\rangle \geq 0.$$

Then with $\frac{1}{4} \leq \theta \leq 1$, it is obvious that the first term in the right side of (34) is also non-negative, hence $\boldsymbol{\mathcal{E}}_{uv}^{h,n+\frac{1}{2}}$ is non-negative. Furthermore, since $\frac{1}{a_1}\|\boldsymbol{W}_h\|^2 \leq \langle \boldsymbol{M}_h \boldsymbol{W}_h, \boldsymbol{W}_h\rangle$ for any $\boldsymbol{W}_h \in V_{h,0}$, we obtain

$$\boldsymbol{\mathcal{E}}_{uv}^{h,n+\frac{1}{2}} \geq \frac{1}{2a_1}\left\|\frac{\boldsymbol{U}_h^{n+1}-\boldsymbol{U}_h^n}{\tau}\right\|^2.$$

2. We now prove the inequality (33). According to (34), we get

$$\boldsymbol{\mathcal{E}}_{uv}^{h,n+\frac{1}{2}} \geq \frac{1}{2}\Big\langle\Big(\boldsymbol{M}_h + (\theta-\frac{1}{4})\tau^2\boldsymbol{A}_h^2\Big)\frac{\boldsymbol{U}_h^{n+1}-\boldsymbol{U}_h^n}{\tau}, \frac{\boldsymbol{U}_h^{n+1}-\boldsymbol{U}_h^n}{\tau}\Big\rangle.$$

Using Lemma 4.3, we obtain

$$\Big\langle \boldsymbol{A}_h^2\frac{\boldsymbol{U}_h^{n+1}-\boldsymbol{U}_h^n}{\tau}, \frac{\boldsymbol{U}_h^{n+1}-\boldsymbol{U}_h^n}{\tau}\Big\rangle \leq \frac{64}{h^4}\left\|\frac{\boldsymbol{U}_h^{n+1}-\boldsymbol{U}_h^n}{\tau}\right\|^2.$$

So, we get

$$\frac{1}{2}(\theta-\frac{1}{4})\tau^2\Big\langle \boldsymbol{A}_h^2\frac{\boldsymbol{U}_h^{n+1}-\boldsymbol{U}_h^n}{\tau}, \frac{\boldsymbol{U}_h^{n+1}-\boldsymbol{U}_h^n}{\tau}\Big\rangle \geq \frac{1}{2a_1}(4\theta-1)\alpha^2\left\|\frac{\boldsymbol{U}_h^{n+1}-\boldsymbol{U}_h^n}{\tau}\right\|^2.$$

Hence it follows

$$\boldsymbol{\mathcal{E}}_{uv}^{h,n+\frac{1}{2}} \geq \frac{1}{2a_1}\left(1+(4\theta-1)\alpha^2\right)\left\|\frac{\boldsymbol{U}_h^{n+1}-\boldsymbol{U}_h^n}{\tau}\right\|^2. \tag{35}$$

With the assumption in (32) the right-hand side of (35) is non-negative, and $\boldsymbol{\mathcal{E}}_{uv}^{h,n+\frac{1}{2}}$ is a non-negative quantity.

□

Proposition 4.2
Let $\boldsymbol{\mathcal{E}}_{uv}^{h,n+\frac{1}{2}}$ be defined as in Proposition 4.1, then for any $n = 0, 1, \ldots, J$, we have the following energy estimation:

$$\sqrt{\boldsymbol{\mathcal{E}}_{uv}^{h,n+\frac{1}{2}}} \leq \sqrt{\boldsymbol{\mathcal{E}}_{uv}^{h,\frac{1}{2}}} + \beta\tau\sum_{k=0}^{n}\|\boldsymbol{M}_h\boldsymbol{f}_h^{k+\theta}\|, \tag{36}$$

with

$$\beta = \begin{cases} \dfrac{\sqrt{2a_1}}{2\sqrt{1+(4\theta-1)\alpha^2}}, & \text{if } 0 \leq \theta < \dfrac{1}{4}, \\ \dfrac{\sqrt{2a_1}}{2}, & \text{if } \dfrac{1}{4} \leq \theta \leq 1. \end{cases}$$

Proof
We write Equation (23), in the following form

$$(\boldsymbol{M}_h + \theta\tau^2\boldsymbol{A}_h^2)\frac{\boldsymbol{U}_h^{n+1}-2\boldsymbol{U}_h^n+\boldsymbol{U}_h^{n-1}}{\tau^2} + \boldsymbol{A}_h\boldsymbol{V}_h^n = \boldsymbol{M}_h\boldsymbol{f}_h^{n+\theta}. \tag{37}$$

Taking the scalar product of (37) with $\dfrac{\boldsymbol{U}_h^{n+1}-\boldsymbol{U}_h^{n-1}}{2\tau}$, leads to

$$\Big\langle(\boldsymbol{M}_h + \theta\tau^2\boldsymbol{A}_h^2)\frac{\boldsymbol{U}_h^{n+1}-2\boldsymbol{U}_h^n+\boldsymbol{U}_h^{n-1}}{\tau^2}, \frac{\boldsymbol{U}_h^{n+1}-\boldsymbol{U}_h^{n-1}}{2\tau}\Big\rangle + \Big\langle\boldsymbol{A}_h\boldsymbol{V}_h^n, \frac{\boldsymbol{U}_h^{n+1}-\boldsymbol{U}_h^{n-1}}{2\tau}\Big\rangle = \Big\langle\boldsymbol{M}_h\boldsymbol{f}_h^{n+\theta}, \frac{\boldsymbol{U}_h^{n+1}-\boldsymbol{U}_h^{n-1}}{2\tau}\Big\rangle, \tag{38}$$

then developing the left-hand side of equation (38), we get

$$\Big\langle (\boldsymbol{M}_h + \theta\tau^2 \boldsymbol{A}_h^2)\frac{\boldsymbol{U}_h^{n+1} - 2\boldsymbol{U}_h^n + \boldsymbol{U}_h^{n-1}}{\tau^2}, \frac{\boldsymbol{U}_h^{n+1} - \boldsymbol{U}_h^{n-1}}{2\tau}\Big\rangle = \frac{1}{2\tau}\Big\langle (\boldsymbol{M}_h + \theta\tau^2 \boldsymbol{A}_h^2)\frac{\boldsymbol{U}_h^{n+1} - \boldsymbol{U}_h^n}{\tau}, \frac{\boldsymbol{U}_h^{n+1} - \boldsymbol{U}_h^n}{\tau}\Big\rangle$$
$$- \frac{1}{2\tau}\Big\langle (\boldsymbol{M}_h + \theta\tau^2 \boldsymbol{A}_h^2)\frac{\boldsymbol{U}_h^{n} - \boldsymbol{U}_h^{n-1}}{\tau}, \frac{\boldsymbol{U}_h^{n} - \boldsymbol{U}_h^{n-1}}{\tau}\Big\rangle. \quad (39)$$

Inserting the Equation (39), into the equation (38), leads to

$$\boldsymbol{\mathcal{E}}_{uv}^{h,n+\frac{1}{2}} - \boldsymbol{\mathcal{E}}_{uv}^{h,n-\frac{1}{2}} = \frac{1}{2}\big\langle \boldsymbol{M}_h \boldsymbol{f}_h^{n+\theta}, \boldsymbol{U}_h^{n+1} - \boldsymbol{U}_h^{n-1}\big\rangle,$$

We then apply the Cauchy-Schwarz inequality, to obtain

$$\begin{aligned}\boldsymbol{\mathcal{E}}_{uv}^{h,n+\frac{1}{2}} - \boldsymbol{\mathcal{E}}_{uv}^{h,n-\frac{1}{2}} &= \frac{1}{2}\big\langle \boldsymbol{M}_h \boldsymbol{f}_h^{n+\theta}, \boldsymbol{U}_h^{n+1} - \boldsymbol{U}_h^{n}\big\rangle + \frac{1}{2}\big\langle \boldsymbol{M}_h \boldsymbol{f}_h^{n+\theta}, \boldsymbol{U}_h^{n} - \boldsymbol{U}_h^{n-1}\big\rangle,\\ &\leq \frac{1}{2}\|\boldsymbol{M}_h \boldsymbol{f}_h^{n+\theta}\| \left(\|\boldsymbol{U}_h^{n+1} - \boldsymbol{U}_h^{n}\| + \|\boldsymbol{U}_h^{n} - \boldsymbol{U}_h^{n-1}\|\right).\end{aligned}$$

- If $0 \leq \theta < \dfrac{1}{4}$, from the inequality (33), we have

$$\sqrt{\boldsymbol{\mathcal{E}}_{uv}^{h,n+\frac{1}{2}}} + \sqrt{\boldsymbol{\mathcal{E}}_{uv}^{h,n-\frac{1}{2}}} \geq \frac{\sqrt{1 + (4\theta - 1)\alpha^2}}{\tau\sqrt{2a_1}} \left(\|\boldsymbol{U}_h^{n+1} - \boldsymbol{U}_h^{n}\| + \|\boldsymbol{U}_h^{n} - \boldsymbol{U}_h^{n-1}\|\right),$$

hence,

$$\boldsymbol{\mathcal{E}}_{uv}^{h,n+\frac{1}{2}} - \boldsymbol{\mathcal{E}}_{uv}^{h,n-\frac{1}{2}} \leq \frac{\tau\sqrt{2a_1}}{2\sqrt{1 + (4\theta - 1)\alpha^2}}\|\boldsymbol{M}_h \boldsymbol{f}_h^{n+\theta}\| \left(\sqrt{\boldsymbol{\mathcal{E}}_{uv}^{h,n+\frac{1}{2}}} + \sqrt{\boldsymbol{\mathcal{E}}_{uv}^{h,n-\frac{1}{2}}}\right),$$

Dividing this inequality by $\sqrt{\boldsymbol{\mathcal{E}}_{uv}^{h,n+\frac{1}{2}}} + \sqrt{\boldsymbol{\mathcal{E}}_{uv}^{h,n-\frac{1}{2}}}$, we get

$$\sqrt{\boldsymbol{\mathcal{E}}_{uv}^{h,n+\frac{1}{2}}} - \sqrt{\boldsymbol{\mathcal{E}}_{uv}^{h,n-\frac{1}{2}}} \leq \frac{\tau\sqrt{2a_1}}{2\sqrt{1 + (4\theta - 1)\alpha^2}}\|\boldsymbol{M}_h \boldsymbol{f}_h^{n+\theta}\|. \quad (40)$$

- For the case $\dfrac{1}{4} \leq \theta \leq 1$, by using inequality (31), and similar arguments as above we obtain

$$\sqrt{\boldsymbol{\mathcal{E}}_{uv}^{h,n+\frac{1}{2}}} - \sqrt{\boldsymbol{\mathcal{E}}_{uv}^{h,n-\frac{1}{2}}} \leq \frac{\tau\sqrt{2a_1}}{2}\|\boldsymbol{M}_h \boldsymbol{f}_h^{n+\theta}\|. \quad (41)$$

Then, using the mathematical induction, both (40) and (41) leads to the inequality (36) for all $n = 0, 1, \ldots, J$, And this ends the proof. □

Definition 4.1
[20] A finite differences scheme is said to be stable in a norm $\|.\|$ if the solution $\boldsymbol{U}_h^n$ satisfies:

$$\|\boldsymbol{U}_h^n\| \leq C,$$

with $C > 0$ is independent of n and h. This implies that the norm of the solution $\boldsymbol{U}_h^n$ remains bounded as $n \to +\infty$ for a fixed h.

Theorem 4.1 (Stability)
Let $\boldsymbol{U}_h^n$ be the numerical solution of the Scheme (23)-(26) and suppose that the initial conditions are sufficiently regular so that $\boldsymbol{\mathcal{E}}_{uv}^{h,\frac{1}{2}} \leq C$, Then we have

1. If $\frac{1}{4} \leq \theta \leq 1$ then the Scheme (23)-(26) is unconditionally stable.
2. If $0 \leq \theta < \frac{1}{4}$ then the Scheme (23)-(26) is stable provided that:

$$\alpha^2 \leq \frac{1}{2}\left(\frac{1}{1-4\theta}\right).$$

Proof

1. If $0 \leq \theta < \frac{1}{4}$ Combining the two inequalities (33) and (36) leads to

$$\sqrt{\frac{(1+(4\theta-1)\alpha^2)}{2a_1}}\left\|\frac{\boldsymbol{U}_h^{n+1}-\boldsymbol{U}_h^n}{\tau}\right\| \leq \sqrt{\boldsymbol{\mathcal{E}}_{uv}^{h,\frac{1}{2}}} + \beta\tau\sum_{k=0}^{n}\left\|\boldsymbol{M}_h\boldsymbol{f}_h^{k+\theta}\right\|. \tag{42}$$

2. If $\frac{1}{4} \leq \theta \leq 1$, similarly using (31) and (36) gives

$$\sqrt{\frac{1}{2a_1}}\left\|\frac{\boldsymbol{U}_h^{n+1}-\boldsymbol{U}_h^n}{\tau}\right\| \leq \sqrt{\boldsymbol{\mathcal{E}}_{uv}^{h,\frac{1}{2}}} + \beta\tau\sum_{k=0}^{n}\left\|\boldsymbol{M}_h\boldsymbol{f}_h^{k+\theta}\right\|. \tag{43}$$

After rearranging, both (42) and (43) can be written as

$$\left\|\boldsymbol{U}_h^{n+1}-\boldsymbol{U}_h^n\right\| \leq 2\beta\tau\sqrt{C_0} + 2\beta^2\tau^2\sum_{k=0}^{n}\left\|\boldsymbol{M}_h\boldsymbol{f}_h^{k+\theta}\right\|.$$

Next, by using the triangle inequality, we get for all $n = 1, \ldots, J$,

$$\left\|\boldsymbol{U}_h^{n}\right\| \leq \left\|\boldsymbol{U}_h^{n-1}\right\| + \left\|\boldsymbol{U}_h^{n}-\boldsymbol{U}_h^{n-1}\right\| \leq \left\|\boldsymbol{U}_h^{n-1}\right\| + 2\beta\tau\sqrt{C_0} + 2\beta^2\tau^2\sum_{k=0}^{n-1}\left\|\boldsymbol{M}_h\boldsymbol{f}_h^{k+\theta}\right\|.$$

Summing this inequality over n starting from 1 leads to

$$\left\|\boldsymbol{U}_h^{n}\right\| \leq \left\|\boldsymbol{U}_h^{0}\right\| + 2\beta n\tau\sqrt{C_0} + 2\beta^2\tau^2\sum_{l=1}^{n}\sum_{k=0}^{l-1}\left\|\boldsymbol{M}_h\boldsymbol{f}_h^{k+\theta}\right\|. \tag{44}$$

We can easily show that $\beta^2 \leq a_1$, providing the CFL condition for the case if $0 \leq \theta < 1/4$. Finally, since $\boldsymbol{U}_h^0 = \bar{\boldsymbol{U}}_h^0$, then $\left\|\boldsymbol{U}_h^0\right\| \leq C$, and we obtain the following desired result

$$\left\|\boldsymbol{U}_h^{n}\right\| \leq \underbrace{\left\|\boldsymbol{U}_h^{0}\right\| + 2\sqrt{a_1}T\sqrt{C_0} + 2a_1T^2\left\|\boldsymbol{M}_h\right\|\max_{0\leq l\leq J}\|\boldsymbol{f}_h^{l+\theta}\|}_{C}. \tag{45}$$

where $C > 0$ is independent of n and h. This ends the proof. □

Theorem 4.2 (Convergence)
Assume that $\tau = \mathcal{O}(h)$, then the solution of the Scheme (23)-(26) converges to the exact solution of the Problem (7)-(8) in the l^2-norm with order $\mathcal{O}(\tau^2 + h^2)$.

Proof
Let (u_{ij}^n, v_{ij}^n) and $(\boldsymbol{U}_h^n, \boldsymbol{V}_h^n)$ be the solutions of the Problem (7)-(8) and the scheme (23)-(26), respectively. Then $(\boldsymbol{u}_h^n, \boldsymbol{v}_h^n)$ at time t_n satisfies:

$$\boldsymbol{M}_h \delta_t^2 \boldsymbol{u}_h^n + \boldsymbol{A}_h \boldsymbol{v}_h^{n+\theta} = \boldsymbol{M}_h \boldsymbol{f}_h^{n+\theta} + \boldsymbol{T}_1^n. \tag{46}$$

On the other hand, $(\boldsymbol{U}_h^n, \boldsymbol{V}_h^n)$ satisfies:

$$\boldsymbol{M}_h \delta_t^2 \boldsymbol{U}_h^n + \boldsymbol{A}_h \boldsymbol{V}_h^{n+\theta} = \boldsymbol{M}_h \boldsymbol{f}_h^{n+\theta}, \tag{47}$$

Defining $\boldsymbol{e}_h^n = \boldsymbol{u}_h^n - \boldsymbol{U}_h^n$, $\boldsymbol{d}_h^n = \boldsymbol{v}_h^n - \boldsymbol{V}_h^n$ as the errors vectors, then subtracting (46) and (47) yields:

$$\boldsymbol{M}_h \delta_t^2 \boldsymbol{e}_h^n + \boldsymbol{A}_h \boldsymbol{d}_h^{n+\theta} = \boldsymbol{T}_1^n, \tag{48}$$

Similarly, by (8) and (24), we obtain

$$\boldsymbol{d}_h^n - \boldsymbol{A}_h \boldsymbol{e}_h^n = \boldsymbol{T}_2^n, \tag{49}$$

Letting $\boldsymbol{\xi}^n = \boldsymbol{d}_h^n - \boldsymbol{A}_h \boldsymbol{T}_2^n$, then we have

$$\begin{cases} \boldsymbol{M}_h \delta_t^2 \boldsymbol{e}_h^n + \boldsymbol{A}_h \boldsymbol{\xi}_h^{n+\theta} = \boldsymbol{T}_1^n - \boldsymbol{A}_h \boldsymbol{T}_2^n, & (50) \\ \boldsymbol{\xi}^n - \boldsymbol{A}_h \boldsymbol{e}_h^n = 0, & (51) \end{cases}$$

We can now employ the stability results obtained in the previous section applied to the system above. We have

$$\boldsymbol{\mathcal{E}}_{uv}^{h,n+\frac{1}{2}} - \boldsymbol{\mathcal{E}}_{uv}^{h,n-\frac{1}{2}} = \frac{1}{2}\big\langle \boldsymbol{T}_1^n - \boldsymbol{A}_h \boldsymbol{T}_2^n, \boldsymbol{e}_h^{n+1} - \boldsymbol{e}_h^{n-1} \big\rangle, \tag{52}$$

then,

$$\begin{aligned} \boldsymbol{\mathcal{E}}_{uv}^{h,n+\frac{1}{2}} - \boldsymbol{\mathcal{E}}_{uv}^{h,n-\frac{1}{2}} &= \frac{1}{2}\big\langle \boldsymbol{T}_1^n, \boldsymbol{e}_h^{n+1} - \boldsymbol{e}_h^{n-1} \big\rangle - \frac{1}{2}\big\langle \boldsymbol{T}_2^n, \boldsymbol{\xi}_h^{n+1} - \boldsymbol{\xi}_h^{n-1} \big\rangle, \\ &= \frac{1}{2}\big\langle \boldsymbol{T}_1^n, \boldsymbol{e}_h^{n+1} - \boldsymbol{e}_h^{n-1} \big\rangle - \frac{1}{2}\big\langle \boldsymbol{T}_2^n, \boldsymbol{\xi}_h^{n+1} + \boldsymbol{\xi}_h^n \big\rangle, + \frac{1}{2}\big\langle \boldsymbol{T}_2^n, \boldsymbol{\xi}_h^n + \boldsymbol{\xi}_h^{n-1} \big\rangle, \end{aligned} \tag{53}$$

Summing up for n from 1 to k in both sides of (53), yields:

$$\boldsymbol{\mathcal{E}}_{uv}^{h,k+\frac{1}{2}} = \boldsymbol{\mathcal{E}}_{uv}^{h,\frac{1}{2}} + \frac{1}{2}\sum_{n=1}^{k} \big\langle \boldsymbol{T}_1^n, \boldsymbol{e}_h^{n+1} - \boldsymbol{e}_h^{n-1} \big\rangle - \frac{1}{2}\big\langle \boldsymbol{T}_2^k, \boldsymbol{\xi}_h^{k+1} + \boldsymbol{\xi}_h^k \big\rangle + \frac{1}{2}\big\langle \boldsymbol{T}_2^1, \boldsymbol{\xi}_h^1 + \boldsymbol{\xi}_h^0 \big\rangle, \tag{54}$$

Using the Cauchy–Schwarz inequality, leads to

$$\boldsymbol{\mathcal{E}}_{uv}^{h,k+\frac{1}{2}} \leq \boldsymbol{\mathcal{E}}_{uv}^{h,\frac{1}{2}} + \frac{1}{2}\sum_{n=1}^{k} \|\boldsymbol{T}_1^n\| \|\boldsymbol{e}_h^{n+1} - \boldsymbol{e}_h^{n-1}\| + \frac{1}{2}\|\boldsymbol{T}_2^k\| \|\boldsymbol{\xi}_h^{k+1} + \boldsymbol{\xi}_h^k\| + \frac{1}{2}\|\boldsymbol{T}_2^1\| \|\boldsymbol{\xi}_h^1 + \boldsymbol{\xi}_h^0\|, \tag{55}$$

According to the Proposition 4.1 and Equation (34), we have, respectively,

$$\|\boldsymbol{e}_h^{n+1} - \boldsymbol{e}_h^n\| \leq \tau \sqrt{2\beta \boldsymbol{\mathcal{E}}_{uv}^{h,n+\frac{1}{2}}}, \text{ and } \|\boldsymbol{\xi}_h^{k+1} + \boldsymbol{\xi}_h^k\|^2 \leq 8 \boldsymbol{\mathcal{E}}_{uv}^{h,k+\frac{1}{2}},$$

substituting these inequalities into (55), yields:

$$\boldsymbol{\mathcal{E}}_{uv}^{h,k+\frac{1}{2}} \leq \boldsymbol{\mathcal{E}}_{uv}^{h,\frac{1}{2}} + + \frac{1}{2}\|\boldsymbol{T}_2^1\| \|\boldsymbol{\xi}_h^1 + \boldsymbol{\xi}_h^0\| + \frac{\sqrt{2\beta}}{2}\tau \sum_{n=1}^{k} \|\boldsymbol{T}_1^n\| \left(\sqrt{\boldsymbol{\mathcal{E}}_{uv}^{h,n+\frac{1}{2}}} + \sqrt{\boldsymbol{\mathcal{E}}_{uv}^{h,n-\frac{1}{2}}} \right) + \sqrt{2}\|\boldsymbol{T}_2^k\| \sqrt{\boldsymbol{\mathcal{E}}_{uv}^{h,k+\frac{1}{2}}}, \tag{56}$$

By means of the two inequalities $ab \leq \frac{1}{2}a^2 + \frac{1}{2}b^2$ and $2ab \leq \frac{1}{\epsilon}a^2 + \epsilon b^2$, we get

$$\boldsymbol{\mathcal{E}}_{uv}^{h,k+\frac{1}{2}} \leq \boldsymbol{\mathcal{E}}_{uv}^{h,\frac{1}{2}} + \frac{1}{2}\|\boldsymbol{T}_2^1\|\|\boldsymbol{\xi}_h^1 + \boldsymbol{\xi}_h^0\| + \frac{\sqrt{2\beta}}{2}\tau\sum_{n=1}^{k}\boldsymbol{\mathcal{E}}_{uv}^{h,n+\frac{1}{2}} + \frac{\sqrt{2\beta}}{2}\tau\sum_{n=0}^{k}\|\boldsymbol{T}_1^n\|^2 + \frac{\sqrt{2}}{2\epsilon}\|\boldsymbol{T}_2^k\|^2 + \frac{\sqrt{2}}{2}\epsilon\boldsymbol{\mathcal{E}}_{uv}^{h,k+\frac{1}{2}}, \tag{57}$$

then we choose ϵ such that $\epsilon \leq \sqrt{2}$, we get

$$\boldsymbol{\mathcal{E}}_{uv}^{h,k+\frac{1}{2}} \leq \boldsymbol{\mathcal{E}}_{uv}^{h,\frac{1}{2}} + \frac{1}{2}\|\boldsymbol{T}_2^1\|\|\boldsymbol{\xi}_h^1 + \boldsymbol{\xi}_h^0\| + \frac{\sqrt{2\beta}}{2}\tau\sum_{n=1}^{k}\boldsymbol{\mathcal{E}}_{uv}^{h,n+\frac{1}{2}} + \frac{\sqrt{2\beta}}{2}\tau\sum_{n=0}^{k}\|\boldsymbol{T}_1^n\|^2 + \frac{\sqrt{2}}{\epsilon}\|\boldsymbol{T}_2^k\|^2. \tag{58}$$

Apply now the Gronwall inequality in Lemma 4.2, to obtain

$$\boldsymbol{\mathcal{E}}_{uv}^{h,k+\frac{1}{2}} \leq C\left(\boldsymbol{\mathcal{E}}_{uv}^{h,\frac{1}{2}} + \|\boldsymbol{T}_2^1\|\|\boldsymbol{\xi}_h^1 + \boldsymbol{\xi}_h^0\| + \tau\sum_{n=0}^{k}\|\boldsymbol{T}_1^n\|^2\right), \tag{59}$$

We now estimate each term in the right hand side of (59). From (25), we have

$$\boldsymbol{e}_h^0 = 0 \ \text{ and } \ \boldsymbol{e}_h^1 = \mathcal{O}(\tau^4) \tag{60}$$

then, $\boldsymbol{\xi}_h^0 = \boldsymbol{A}_h\boldsymbol{e}_h^0 = 0$ and $\|\boldsymbol{\xi}_h^1\| = \|\boldsymbol{A}_h\boldsymbol{e}_h^1\| \leq \frac{C}{h^2}\|\boldsymbol{e}_h^1\|$. With $\tau = \mathcal{O}(h)$, we get

$$\|\boldsymbol{\xi}_h^1\| \leq Ch^2. \tag{61}$$

For the term $\boldsymbol{\mathcal{E}}_{uv}^{h,\frac{1}{2}}$, by definition we have

$$\boldsymbol{\mathcal{E}}_{uv}^{h,\frac{1}{2}} = \frac{1}{2}\Big\langle(\boldsymbol{M}_h + \theta\tau^2\boldsymbol{A}_h^2)\frac{\boldsymbol{e}_h^1 - \boldsymbol{e}_h^0}{\tau}, \frac{\boldsymbol{e}_h^1 - \boldsymbol{e}_h^0}{\tau}\Big\rangle + \frac{1}{2}\langle\boldsymbol{\xi}_h^0, \boldsymbol{\xi}_h^1\rangle,$$

It follows,

$$\boldsymbol{\mathcal{E}}_{uv}^{h,\frac{1}{2}} \leq \frac{a_0}{2}\left\|\frac{\boldsymbol{e}_h^1 - \boldsymbol{e}_h^0}{\tau}\right\|^2 + \frac{\theta}{2}\|\boldsymbol{\xi}_h^1 - \boldsymbol{\xi}_h^0\|^2,$$

Combining (60) and (61), yields:

$$\boldsymbol{\mathcal{E}}_{uv}^{h,\frac{1}{2}} \leq C((\tau^3)^2 + (h^2)^2), \tag{62}$$

For the other terms, We recall that

$$\|\boldsymbol{T}_2^1\| \leq Ch^2 \text{ and } \|\boldsymbol{T}_1^n\| \leq C(\tau^2 + h^2),$$

then,

$$\|\boldsymbol{T}_2^1\|\|\boldsymbol{\xi}_h^1 + \boldsymbol{\xi}_h^0\| \leq C(h^2)^2 \text{ and } \tau\sum_{n=0}^{k}\|\boldsymbol{T}_1^n\|^2 \leq C(\tau^2 + h^2)^2 \tag{63}$$

Substituting (62)-(63) into (59) , we obtain

$$\boldsymbol{\mathcal{E}}_{uv}^{h,k+\frac{1}{2}} \leq C(\tau^2 + h^2)^2. \tag{64}$$

Finally, since

$$\|\boldsymbol{e}_h^{n+1} - \boldsymbol{e}_h^n\| \leq \tau\sqrt{2\beta\boldsymbol{\mathcal{E}}_{uv}^{h,n+\frac{1}{2}}},$$

then,

$$\begin{aligned}\|\boldsymbol{e}_h^{n+1}\| &\leq \|\boldsymbol{e}_h^n\| + \|\boldsymbol{e}_h^{n+1} - \boldsymbol{e}_h^n\|,\\ &\leq \|\boldsymbol{e}_h^n\| + \tau\sqrt{2\beta\boldsymbol{\mathcal{E}}_{uv}^{h,n+\frac{1}{2}}}\end{aligned} \tag{65}$$

Summing up for n from 0 to k in both sides of (65), yields:

$$\|\boldsymbol{e}_h^{k+1}\| \leq \tau\sum_{n=0}^{k}\sqrt{2\beta\boldsymbol{\mathcal{E}}_{uv}^{h,n+\frac{1}{2}}} \tag{66}$$

which implies, by using (64),

$$\|\boldsymbol{e}_h^{k+1}\| \leq C(\tau^2 + h^2). \tag{67}$$

This completes the proof. □

5. Restricted additive Schwarz preconditioner

Applying the method (23)-(26) to solve the plate equation (1) leads at every time step to a linear system of the form

$$\boldsymbol{\mathcal{Q}}_h\boldsymbol{U}_h = \boldsymbol{b}_h, \tag{68}$$

which the associated matrix $\boldsymbol{\mathcal{Q}}_h$ is given by:

$$\boldsymbol{\mathcal{Q}}_h = \boldsymbol{M}_h + \theta\tau^2\boldsymbol{A}_h^2.$$

For such discretization, it's well established that the condition number κ of $\boldsymbol{\mathcal{Q}}_h$ satisfies : $\kappa = \mathcal{O}(h^{-4})$ (see [19]), thus growing fast and unboundedly when the mesh size h tend to 0. Our aim in this section is to construct and apply the restricted additive Schwarz preconditioner for $\boldsymbol{\mathcal{Q}}_h$.

In order to apply the restricted additive Schwarz preconditioner, the domain $\Omega \subset \mathbb{R}^2$ will be decomposed into p non-overlapping subdomains $\widehat{\Omega}_i$, $i = 1, \ldots, p$, such that $\Omega = \bigcup_{i=1}^{p}\widehat{\Omega}_i$. The overlapping decomposition of Ω is obtained using the following definition:

$$\Omega_i \coloneqq \{x \in \Omega \ / \ dist(x, \widehat{\Omega}_i) \leq \delta\}.$$

where the parameter δ is the width of the overlap between the subdomains Ω_i. The overlapping subdomains Ω_i, $i = 1, \ldots, p$, satisfies

$$\Omega = \bigcup_{i=1}^{p}\Omega_i.$$

See, the Figure 1 (from [8]) for an example of a non overlapping decomposition (left) and overlapping decomposition (right) of the domain Ω.

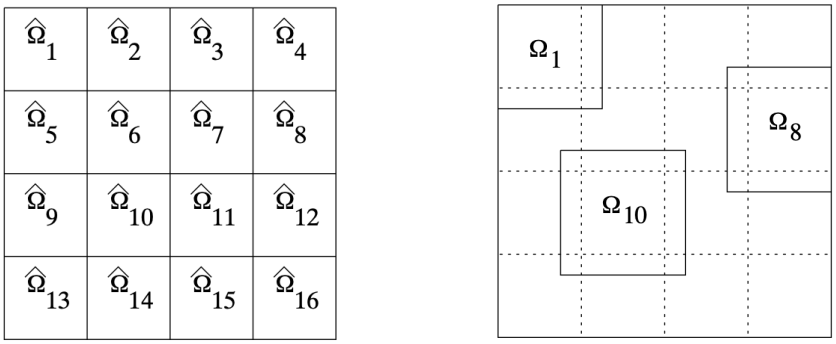

Figure 1. *Left:* Domain partition without overlap for 16 subdomains. *Right:* The 16 subdomains with overlap.

Let us denote by q the size of the discretization matrix $\boldsymbol{\mathcal{Q}}_h$ and let $\mathcal{I} = \{1, \ldots, q\}$ be the set of all indices of the grid points inside Ω. Similarly we let for each $1 < i < p$, $\mathcal{I}_i$ denotes the set of all indices of the grid points in the interior of Ω_i. The cardinality of the set $\mathcal{I}_i$ is denoted by n_i. Note that, since $\{\Omega_i\}_{i=1}^p$ form an overlapping decomposition of Ω It follows that

$$\mathcal{I}_i \cap \mathcal{I}_j \neq \emptyset, \ \forall i \neq j, \text{ and } \mathcal{I} = \bigcup_{i=1}^{p} \mathcal{I}_i.$$

We then, define the submatrix A_i of size $n_i \times n_i$ corresponding to the subdomain Ω_i, using the following relation:

$$A_i = R_i A R_i^T,$$

where R_i is the restriction matrix, i.e., a $n_i \times q$ rectangular matrix such that for any vector $v \in \mathbb{R}^q$, $R_i v \in \mathbb{R}^{n_i}$ is a vector whose entries correspond to the values of v at grid points in the interior of the subdomain Ω_i.
The transpose R_i^T of R_i is defined by: For any vector $v \in \mathbb{R}^{n_i}$, we have

$$\left(R_i^T v\right)_j = v_j, \text{ if } j \in \mathcal{I}_i \text{ and } \left(R_i^T v\right)_j = 0, \text{ if } j \notin \mathcal{I}_i.$$

We also introduce the rectangular matrix R_i^0, which restricts now a full vector v in $\mathbb{R}^q$, to a subvector whose entries corresponds to the values of v at grid points in the interior of the subdomain $\widehat{\Omega_i}$, hence excluding the grid points inside the overlapping region.
Defining

$$P_{ras}^{-1} = \sum_{i=1}^{p} (R_i^0)^T A_i^{-1} R_i,$$

Then, the Restricted additive Schwarz method for Equation (68) consists of solving the following preconditioned linear system:

$$P_{ras}^{-1} Q_h \boldsymbol{U}_h = P_{ras}^{-1} g_h, \tag{69}$$

By using an iterative method. Since the new system matrix $P_{ras}^{-1} Q_h$ is not symmetric, we choose to use the GMRES method as an acceleration method. Note that the preconditioner P_{ras}^{-1} is not assembled explicitly; instead, we only need to compute its action on any given vector, which is achieved by the following algorithm:

Algorithm 1: Restricted Additive Schwarz Preconditioner

input : v

Do in parallel for each subdomain Ω_i*:*

$b_i \longleftarrow R_i v$

solve the linear system: $A_i x_i = b_i$

$w_i \longleftarrow (R_i^0)^T x_i$

Sum:

$$P_{ras}^{-1} v \longleftarrow \sum_{i=1}^{p} w_i$$

output: $P_{ras}^{-1} v$

Remark 5.1
In a parallel computing environment, each processor (or core) i, $(1 \leq i \leq p)$ will be charged to solve using direct method a linear system associated with the subdomain Ω_i.

6. Numerical experiments

To validate the performance of the scheme and the RAS algorithm presented in this work, two numerical examples are considered. In the following we calculated the l^2 and l^∞ errors via the formulas:

$$\|\boldsymbol{e}_h^n\|_\infty = \max_{1\leq i,j\leq N-1} |u_{ij}^n - U_{ij}^n|, \text{ and } \|\boldsymbol{e}_h^n\|_2 = h\sqrt{\sum_{ij=1}^{N-1} |u_{ij}^n - U_{ij}^n|^2},$$

The order of convergence of the present scheme is computed via the formula:

$$Order = \frac{\log\left(\|\boldsymbol{e}_{s_1}\|/\|\boldsymbol{e}_{s_2}\|\right)}{\log\left(s_1/s_2\right)},$$

where $\|\boldsymbol{e}_{s_1}\|$ and $\|\boldsymbol{e}_{s_2}\|$ are the errors for the mesh of sizes s_1 and s_2, respectively, and $\|.\|$ is either the l^2 or the l^∞ norm.

The linear system (68), at every time step, is solved iteratively by the preconditioned GMRES method, using the restricted additive Schwarz preconditioner. The stopping criterion is to bring the relative residual under $tol = 10^{-9}$. All experiments presented in this section were obtained using MATLAB R2022a on a MacBook computer equipped with a 2.3 GHz, 8GB of RAM, Intel Core i5. For the implementation of the parallel domain decomposition algorithm we have used the parallel computing toolbox (PCT) included in MATLAB. Each subdomain's linear system is assigned to one processor core and solved using MATLAB's backslash operator.

Problem 1

We consider homogeneous plate Equation (1) with $a(x, y) = 1$, $\Omega = [0, 1]^2$, $T = 1$. The applied transverse loading f is:

$$f(x, y, t) = (\pi^2 + 64\pi^4)\exp(-\pi t)\sin(2\pi x)\sin(2\pi y),$$

the analytic solution is

$$u(x, u, t) = \exp(-\pi t)\sin(2\pi x)\sin(2\pi y).$$

Figure 2, left, shows the numerical solution surface obtained by the present scheme at $T = 1$ with $h = 1/64$, $\tau = 0.0016$ and $\theta = 1/4$. The agreement with the exact solution (plotted in the right of the same figure) is seen to be very good.

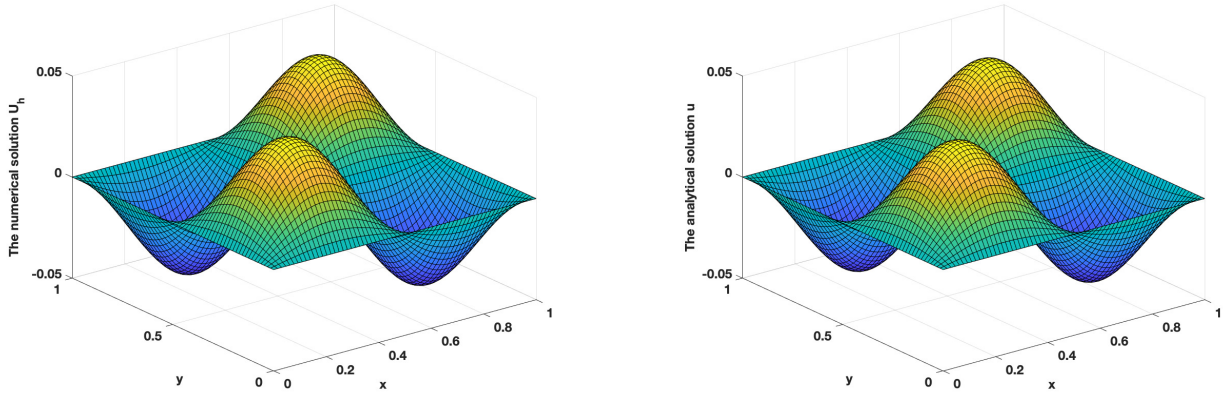

Figure 2. Left: The numerical solution U_h of Problem 1 with $h = 1/64$ and $\tau = 0.0016$, $\theta = 1/4$ at $T = 1$. Right: The analytical solution u of Problem 1 at $T = 1$

Table 2 shows the l^2 and l^∞ errors and the spatial convergence orders of the numerical solution U_h obtained in solving Problem 1 for different values of the mesh size h and $\tau = 0.0004$, $\theta = 1/4$ at $T = 1$, using the present scheme. It can be seen that as $h \to 0$ the numerical solution converges to the analytical solution. The experimental order of space convergence is almost 2, which is in accord with the theoretical order. In Table 3, we present the experiment results in solving Problem 1 for different values of the time step τ, with fixed $h = 1/256$, and $\theta = 1/2$ at $T = 1$, which confirms that the present scheme has order two in time.

Table 2. Errors and convergence orders in space for Problem 1 with $\tau = 0.0004$ and $\theta = 1/4$ at $T = 1$

h	$l^\infty - Error$	*Order*	$l^2 - Error$	*Order*
$\frac{1}{16}$	2.2507×10^{-02}	—	1.1253×10^{-02}	—
$\frac{1}{32}$	6.6445×10^{-03}	1.760109	3.3223×10^{-03}	1.760112
$\frac{1}{64}$	1.5826×10^{-03}	2.069908	7.9128×10^{-04}	2.069905
$\frac{1}{128}$	3.8756×10^{-04}	2.029763	1.9378×10^{-04}	2.029764
Average		1.953260		1.953260

Table 3. Errors and convergence orders in time for Problem 1 with $h = 1/256$ and $\theta = 1/2$ at $T = 1$

τ	$l^\infty - Error$	*Order*	$l^2 - Error$	*Order*
$\frac{1}{10}$	7.0300×10^{-02}	—	3.5150×10^{-02}	—
$\frac{1}{20}$	2.0106×10^{-02}	1.805901	1.0053×10^{-02}	1.805901
$\frac{1}{40}$	5.8481×10^{-03}	1.781586	2.9240×10^{-03}	1.781586
$\frac{1}{80}$	1.2789×10^{-03}	2.192999	6.3947×10^{-04}	2.192999
Average		1.9268		1.9268

For comparison purposes, we solve the linear system (68) at every time step by the GMRES method without a preconditioner. Then, we apply the restricted additive Schwarz preconditioner associated with 4 subdomains with an overlap width $\delta = 0.1$. In Table 4 we list the condition number values when solving Problem 1, showing that it increases as $\mathcal{O}(h^{-4})$.

Table 4. Without preconditioner: Growth of the condition number for Problem 1 with $\tau = 0.0016$, $\delta = 0.1$, $p = 4$, $\theta = 1/2$ at $T = 1$

h	*Condition number*	*Rate*
$\frac{1}{16}$	$6.0192 \times 10^{+00}$	$--$
$\frac{1}{32}$	$8.2487 \times 10^{+01}$	-3.7765
$\frac{1}{64}$	$1.3095 \times 10^{+03}$	-3.9887
$\frac{1}{128}$	$2.0956 \times 10^{+04}$	-4.0003
Average		-3.9218

The condition number, the number of iterations and CPU time (in seconds) for the RAS preconditioned method and the unpreconditioned method are given in Table 5, for different mesh sizes h and $\tau = 0.0004$ at time step $T = 1$. One can see that as h decreases, the condition number grows fast and unboundedly for the unpreconditioned case. As a consequence the number of iterations and CPU time for the RAS method are significantly lesser than those for the unpreconditioned case, which show the effectiveness of the RAS method.

Table 5. Condition number, GMRES iterations and CPU time for solving the Problem 1 with $\tau = 0.0016$, $\delta = 0.1$, $p = 4$ and $\theta = 1/2$ at $T = 1$

h	*without preconditioner*			*RAS preconditioner*		
	Condition number	*Iteration*	*CPU Time (s)*	*Condition number*	*Iteration*	*CPU Time (s)*
$\frac{1}{16}$	$6.0192 \times 10^{+00}$	3	2.2558×10^{-01}	$1.3302 \times 10^{+00}$	6	4.4275×10^{-01}
$\frac{1}{32}$	$8.2487 \times 10^{+01}$	12	3.8850×10^{-01}	$1.6238 \times 10^{+00}$	7	$6.4997 \times 10^{+00}$
$\frac{1}{64}$	$1.3095 \times 10^{+03}$	44	$9.2983 \times 10^{+00}$	$3.3950 \times 10^{+00}$	7	$3.3499 \times 10^{+01}$
$\frac{1}{128}$	$2.0956 \times 10^{+04}$	165	$2.6886 \times 10^{+02}$	$2.2535 \times 10^{+01}$	8	$1.9041 \times 10^{+02}$

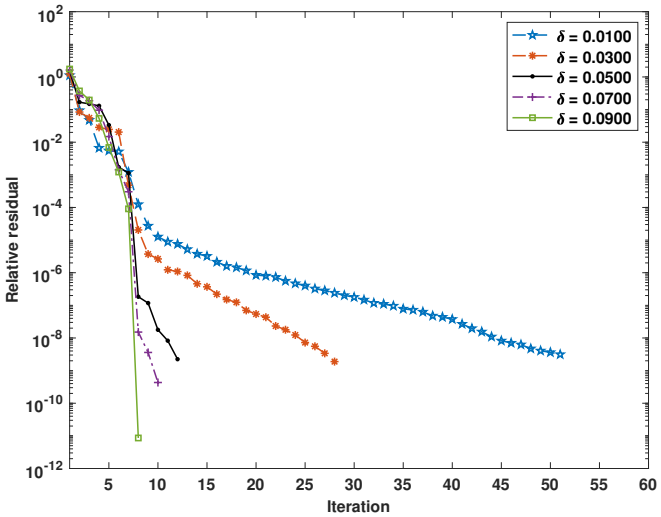

Figure 3. Problem 1: Convergence history of the GMRES method using RAS preconditioner for different overlap widths δ, $p = 2$, $h = 1/64$, and $\tau = 0.015$

In Figure 3, we show the number of iterations to achieve a relative residual error lesser than 10^{-9} for the restricted additive Schwarz preconditioner applied with different overlap sizes δ to solve Problem 1. The obtained results show that the RAS algorithm performs better for bigger δ, since the RAS algorithm converges in less iterations in this case.

Problem 2

We consider a thin plate occupying the domain $\Omega = [0,1]^2$, the transverse deflection u is governed by equation (1), we let $a(x,y) = 1 + x^2 + y^2$, $T = 1$, and the applied transverse loading is given by:

$$f(x,y,t) = (1 + 4\pi^4(1 + x^2 + y^2))\sinh(t)\sin(\pi x)\sin(\pi y).$$

The analytic solution is given by

$$u(x,u,t) = \sinh(t)\sin(\pi x)\sin(\pi y).$$

Figure 4, shows the good agreement of the numerical solution ($h = 1/64$ at $T = 1$) obtained by our proposed scheme with the analytical solution.

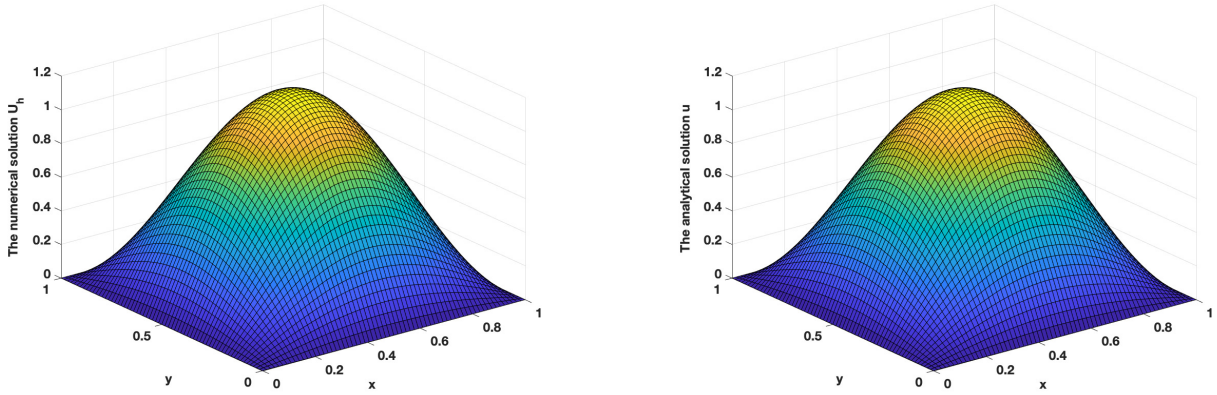

Figure 4. Left: The numerical solution U_h of Problem 2 with $h = 1/64$ and $\tau = 0.0016$, $\theta = 1/4$ at $T = 1$. Right: The analytical solution u of Problem 2 at $T = 1$

Similar to Problem 1, we let $T = 1$, then we solve the Problem 2 by the present scheme for different values of the mesh size h and for $\theta = 1/8$. In this case ($0 \leq \theta < 1/4$) the time step τ is chosen, in order to fulfill the CFL restriction. The l^2 and l^∞ errors and the spatial convergence orders for Problem 2 are reported in Table 6. Again, with h approaching zero, the numerical solution converges to the analytical solution, and the experimental order of space convergence is almost 2, which is in accord with the theoretical order.

Table 6. Errors and convergence orders in space for Problem 2 with $\theta = 1/8$ at $T = 1$

h	$l^\infty - Error$	*Order*	$l^2 - Error$	*Order*
$\frac{1}{16}$	7.7739×10^{-03}	—	3.8869×10^{-03}	—
$\frac{1}{32}$	1.9358×10^{-03}	2.005680	9.6788×10^{-04}	2.005717
$\frac{1}{64}$	4.8347×10^{-04}	2.001457	2.4173×10^{-04}	2.001449
$\frac{1}{128}$	1.2084×10^{-04}	2.000340	6.0418×10^{-05}	2.000337
Average		2.002492		2.002501

Table 7. Errors and convergence orders in time for Problem 2 with $h = 1/256$ and $\theta = 1/2$ at $T = 1$

τ	$l^\infty - Error$	*Order*	$l^2 - Error$	*Order*
$\frac{1}{10}$	5.5315×10^{-03}	—	2.7660×10^{-03}	—
$\frac{1}{20}$	1.4132×10^{-03}	1.968697	7.0669×10^{-04}	1.968629
$\frac{1}{40}$	3.4516×10^{-04}	2.033649	1.7258×10^{-04}	2.033829
$\frac{1}{80}$	6.4388×10^{-05}	2.422384	3.2193×10^{-05}	2.422423
Average		2.141576		2.141627

In Table 7, we present the numerical results in solving Problem 2 for different values of the time step τ, with fixed $h = 1/256$, and $\theta = 1/2$ at $T = 1$. As we can see, the present scheme has order two in time. In Table 8, we compare our algorithm (RAS preconditioner) with the Additive Schwarz (AS) preconditioner studied in [19] and the ILU(0) preconditioner. We take $\tau = 0.01$, $tol = 10^{-12}$, $\theta = 1/2$ and $T = 1$. As can be seen in these results, when h decreases (i.e., when the size of the problem increases) the number of iterations and CPU time for the RAS method are significantly better compared to those of the Additive Schwarz case and to those of ILU(0) case. We note that when solving the Problem 2 for $h = 1/512$, the ILU(0) method cant reaches the stopping criterion, which is not the case with the RAS method.

Table 8. GMRES iterations and CPU time for solving the Problem 2 with $\tau = 0.01$ $\delta = 0.35$, $p = 2$ and $\theta = 1/2$ at $T = 1$

h	*RAS preconditioner*		*AS preconditioner*		*ILU(0) preconditioner*	
	Iteration	*CPU Time (s)*	*Iteration*	*CPU Time (s)*	*Iteration*	*CPU Time (s)*
$\frac{1}{192}$	10	$1.0871 \times 10^{+02}$	11	$1.1877 \times 10^{+02}$	17	$1.0255 \times 10^{+02}$
$\frac{1}{256}$	10	$1.7949 \times 10^{+02}$	12	$2.1344 \times 10^{+02}$	22	$3.0949 \times 10^{+02}$
$\frac{1}{320}$	10	$3.4932 \times 10^{+02}$	12	$4.1794 \times 10^{+02}$	30	$7.0410 \times 10^{+02}$
$\frac{1}{384}$	10	$4.7692 \times 10^{+02}$	12	$5.7277 \times 10^{+02}$	45	$1.6079 \times 10^{+03}$
$\frac{1}{512}$	10	$1.3746 \times 10^{+03}$	12	$1.5871 \times 10^{+03}$	$--$	$--$

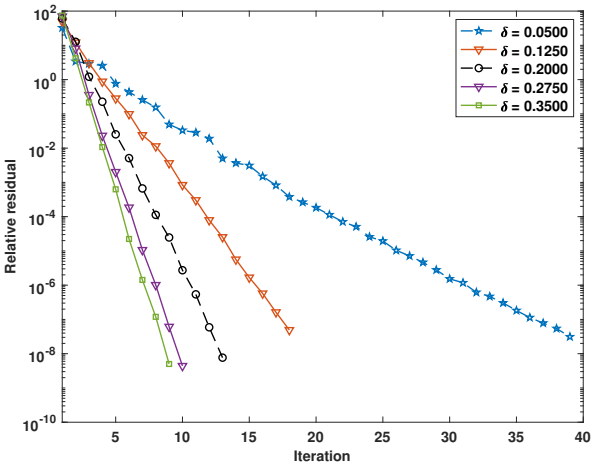

Figure 5. Problem 2: Convergence history of the GMRES method using RAS preconditioner for different overlap widths δ, $p = 2$, $h = 1/64$, and $\tau = 0.015$

We present in Figure 5, the number of iterations of GMRES method combined with the the restricted additive Schwarz preconditioner for different overlap widths δ to solve Problem 2. The obtained results show again that the RAS method performs better with bigger δ.

7. Concluding remarks

A two-dimensional 4th-order variable coefficient PDE governing the vibrations of a simply supported thin plate is studied in this paper. We first established some a priori estimates for the weak approximation of the solution of (1), then we presented a finite difference spatial scheme combined with a θ time scheme to solve our problem. We studied the stability and convergence using the energy method since Fourier analysis cant easily handle variable coefficient problems. Numerical analysis and experiments show that the present scheme is unconditionally stable and convergent in the l^2 norm when $1/4 \leq \theta \leq 1$, and it is conditionally stable and convergent in the l^2-norm under the CFL restriction when $0 \leq \theta < 1/4$. The convergence order is two in both temporal and spatial variables. To precondition the discrete approximations of the problem (1) obtained using our scheme, we used the restricted additive Schwarz preconditioner for the GMRES method. This parallel preconditioning technique improves significantly the condition numbers and speed up the solution process when the size of the linear system increases as shown by the numerical experiments reported in section 6. We are currently working to extend this technique to solve three-dimensional biharmonic equation and nonlinear 4th-order PDE.

REFERENCES

[1] M. D. Aouragh, Y. Khali, S. Khallouq, and M. Segaoui. *Compact finite difference scheme for euler-bernoulli beam equation with a simply supported boundary conditions*. International Journal of Applied and Computational Mathematics, vol. 10, 2024.

[2] T. Aziz, A. Khan, and J. Rashidinia. *Spline methods for the solution of 4th-order parabolic partial differential equations*. Applied Mathematics and Computation, vol. 167, pp. 153–166, 2005.

[3] H. Belhadj, M. Fihri, S. Khallouq, and N. Nagid. *Optimal number of schur subdomains: Application to semi-implicit finite volume discretization of semilinear reaction diffusion problem*. Discrete and Continuous Dynamical Systems - S, vol. 11, pp. 21–34, 2018.

[4] H. Belhadj, S. Khallouq, and M. Rhoudaf. *Parallelization of a finite volumes discretization for anisotropic diffusion problems using an improved schur complement technique*. Discrete and Continuous Dynamical Systems - S, vol. 14, pp. 2075–2099, 2021.

[5] A. Ben bouzid, Y. Khali, and S. Khallouq. *A new algorithm coupling Schwarz domain decomposition and high-order compact finite difference to solve an Euler-Bernoulli beam equation with variable coefficients*. In: Ashraf, M., Al Jaraden, J., Oukhtite, L., El Kinani, E.H. (eds) Algebra and Differential Equations with Applications. SICMA 2023. Springer Proceedings in Mathematics & Statistics, vol. 508, pp. 271—289, 2025.

[6] A. Ben bouzid, Y. Khali, S. Khallouq, and N. Nagid. *Accelerated restricted additive schwarz method for asynchronous processing*. Results in Applied Mathematics, vol. 26, 2025.

[7] A. Ben bouzid, S. Khallouq, and N. Nagid. *A parallel time-Schwarz domain decomposition method applied to an Euler-Bernoulli beam equation with constant coefficients*. Mathematical Foundations of Computing, vol. 11, pp. 32–51, 2026.

[8] S. C. Brenner. *Lower bounds for two-level additive schwarz preconditioners with small overlap*. SIAM Journal on Scientific Computing, vol. 21, pp. 1657–1669, 2000.

[9] H. Caglar and N. Caglar. *Fifth-degree b-spline solution for a 4th-order parabolic partial differential equations*. Applied Mathematics and Computation, vol. 201, pp. 597–603, 2008.

[10] X.-C. Cai and M. Sarkis. *A restricted additive schwarz preconditioner for general sparse linear systems*. SIAM Journal on Scientific Computing, vol. 21, pp. 792–797, 1999.

[11] X. Chang and H. Li. *A pod-based reduced-dimension method for solution coefficient vectors in the crank–nicolson mixed finite element method for the 4th-order parabolic equation*. Fractal and Fractional, vol. 9, 2025.

[12] I. Chueshov and I. Lasiecka. *Existence, uniqueness of weak solutions and global attractors for a class of nonlinear 2d kirchhoff-boussinesq models*. Discrete and Continuous Dynamical Systems, vol. 15, pp. 777–809, 2006.

[13] S. D. Conte. *A stable implicit finite difference approximation to a fourth order parabolic equation*. J. ACM, vol. 4, pp. 18–23, 1957.

[14] S. H. Crandall. *Numerical treatment of a fourth order parabolic partial differential equation*. J. ACM, vol. 1, pp. 111–118, 1954.

[15] V. Dolean, P. Jolivet, and F. Nataf. An Introduction to Domain Decomposition Methods. Society for Industrial and Applied Mathematics, Philadelphia, PA, 2015.

[16] M. Dryja and O. B. Widlund. *Chapter 16 - some domain decomposition algorithms for elliptic problems*. In D. R. Kincaid and L. J. Hayes, editors, Iterative Methods for Large Linear Systems, Academic Press, pp. 273–291, 1990.

[17] E. Efstathiou and M. J. Gander. *Why restricted additive schwarz converges faster than additive schwarz*. BIT Numerical Mathematics, vol. 43, pp. 945–959, 2003.

[18] G. Fairweather and A. R. Gourlay. *Some stable difference approximations to a fourth-order parabolic partial differential equation*. Comput. Math, vol. 21, pp. 1–11, 1977.

[19] Y. Khali, S. Khallouq, and N. Nagid. *Parallel Additive Schwarz Preconditioner for a Discrete Nonlinear Plate Vibration Problem Using a θ-Scheme in Time and Finite Difference in Space* . Mathematical Methods in the Applied Sciences, vol. 48, pp. 14990–15014, 2025.

[20] H.-O. Kreiss. *Initial boundary value problems for hyperbolic systems*. Communications on Pure and Applied Mathematics, vol. 23, pp. 277–298, 1970.

[21] Q. Li, Q. Yang, and H. Chen. *Compact difference scheme for two-dimensional 4th-order nonlinear hyperbolic equation*. Numerical Methods for Partial Differential Equations, vol. 36, pp. 1938–1961, 2020.

[22] Q. Li, H. Chen, and H. Wang. *A proper orthogonal decomposition-compact difference algorithm for plate vibration models*. Numerical Algorithms, vol. 94, pp. 1489–1518, 2023.

[23] H.-L. Liao and Z.-Z. Sun. *Maximum norm error bounds of adi and compact adi methods for solving parabolic equations*. Numerical Methods for Partial Differential Equations, vol. 26, pp.37–60, 2010.

[24] T. P. A. Mathew. *Domain Decomposition Methods for the Numerical Solution of Partial Differential Equations*. Springer Berlin, Heidelberg, vol. 61, 2008.

[25] R. C. Mittal, S. Kumar, and R. Jiwari. *A comparative study of cubic b-spline-based quasi-interpolation and differential quadrature methods for solving fourth-order parabolic pdes*. Proceedings of the National Academy of Sciences, India Section A: Physical Sciences, vol. 91, pp. 461–474, 2021.

[26] R. Mohammadi. *Sextic b-spline collocation method for solving euler–bernoulli beam models*. Applied Mathematics and Computation, vol. 241, pp. 151–166, 2014.

[27] R. Mohanty and D. Kaur. *Unconditionally stable high accuracy compact difference schemes for multi-space dimensional vibration problems with simply supported boundary conditions*. Applied Mathematical Modelling, vol. 55, pp. 281–298, 2018.

[28] J. Park. *Additive Schwarz Methods for Fourth-Order Variational Inequalities*. J Sci Comput 101, 74, 2024.

[29] A. Quarteroni and A. Valli. Domain decomposition methods for partial differential equations. Oxford University Press, 1999.

[30] A. Toselli and O. Widlund. Domain decomposition methods-algorithms and theory, Springer Science & Business Media, vol. 34, 2004.

[31] E. Twizell and A. Khaliq. *A difference scheme with high accuracy in time for fourth-order parabolic equations*. Computer Methods in Applied Mechanics and Engineering, vol. 41, pp. 91–104, 1983.

[32] X. Wang and W. Dai. *A conservative fourth-order stable finite difference scheme for the generalized rosenau–kdv equation in both 1d and 2d*. Journal of Computational and Applied Mathematics, vol. 355, pp. 310–331, 2019.